JOURNAL OF MATERIALS SCIENCE **38** (2003) 3669–3675

Simulation of liquid infiltration and semi-solid extrusion for composite tubes by quasi-coupling thermal-mechanical finite element method

LE-HUA QI, ZHONG-KE SHI, HE-JUN LI, PEI-LING CUI, HONG-MEI HAN
Department of Mechanical Engineering and Automatization, College of Mechanical and Electric Engineering, Northwestern Polytechnical University, Xi'an 710072, People's Republic of China
E-mail: lihejun@nwpu.edu.cn

As a new metal forming technology, the liquid infiltration and semi-solid extrusion process can produce various composite parts, such as tubes, bars, and shaped products, in a single process. In this paper, the liquid infiltration and semi-solid extrusion process for forming a composite tube is simulated by means of thermal rigid-plastic quasi-coupling FEM method. The key technologies such as the handling of liquid phase zone, the transition between liquid and solid phase zones, the grid re-meshing method and the establishment of the boundary condition have also been studied. Based on the FEM simulation software developed by the authors and the grid re-meshing technology, the distribution of stress field, strain field and deformation force in the liquid infiltration and semi-solid extrusion process for forming composite tubes are obtained. The deformation force simulation results accord with the experimental data, indicating the reliability of the system. Therefore, the present research is theoretically valuable in the product quality control and the process parameter choice.

1. Introduction

The tube, bar and other shaped products of metal matrix composites can't be produced directly by present technologies, such as, the hot press diffusion method, the powder method, the infiltration casting method and the liquid metal forging method [1–3]. It needs a second deforming process to produce these kinds of products by the methods mentioned above, i.e., producing the composite blanks first and then the composite tube, bar and other shaped products are produced by extruding or rolling process. However, the new forming technology, liquid infiltration and semi-solid extrusion (LISSE for short), succeeds in producing the composite products in a single process. Rather the composite parts are formed directly from liquid metal after the fiber preforms being prepared. Obviously the cost is cut down greatly [4]. As illustrated in Fig. 1, the first step is to prepare fiber preforms and melt the alloy, and the next is to pour the liquid metal into the container with the fiber preform inside, then fall down the punch to exert and keep pressure on the liquid metal, which forces the liquid metal to impregnate into the fiber preform. After that, the punch starts to fall down again to exert higher pressure on the liquid metal or the semi-solid metal that has been impregnated in the preform, thus the needed workpiece will be extruded out from the outlet of the forming die continually. Obviously, this technology is applicable in many fields. While, the qualified composite workpiece are available under lower pressure by keeping the metal inside the forming die in semi-solid state, as well as the metal inside the container in liquid state, and simultaneously no liquid metal extruded out from the outlet of the forming die. Being related with such technologies as infiltration under pressure, transition from liquid metal to solid metal and semi-solid deformation, it is of great difficulty to apply the technology practically. On the other hand, the pressure of liquid infiltration, the infiltration time, the deformation force in semi-solid state, the preheating temperature of the fiber preform and other process parameters will all affect the infiltration effect, the composite forming quality and the mechanical performance. So it is important to study the flow rule of the liquid metal and the semi-metal metal, the deformation rule of the solid metal and the transpositional rule of the temperature fields for the rational choice of the process parameters, and for the control of forming process and workpiece forming quality.

Although there are many successful cases to analyze and simulate the forming process of solid metal by adopting the rigid-plastic finite element method (FEM) [5–7], there are few cases to simulate and study the forming process of the composite tubes coupling with solidification, heat exchanging and large plastic deformation processes. In this paper, the forming process of the LISSP for forming Al_2O_{3sf}/Al alloy composite tubes is simulated by adopting quasi-coupling thermal-rigid-plastic FEM, and the temperature fields during

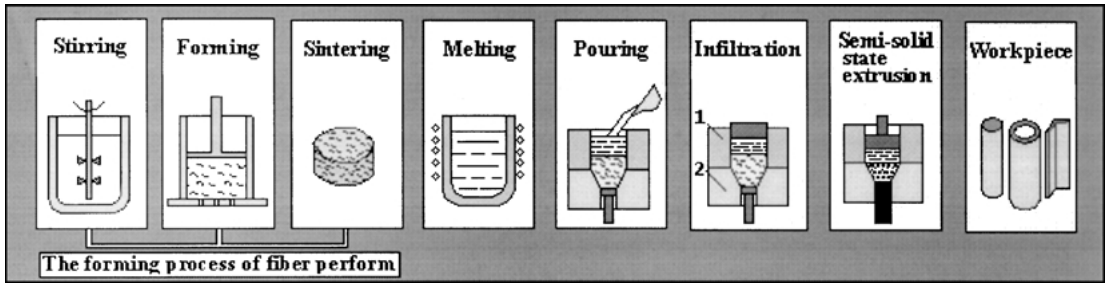

Figure 1 Scheme of the composite forming process by liquid infiltration and semi-solid extrusion: (1) extrusion container and (2) forming die.

extrusion, the stress-strain fields and deformation force are obtained, the result coincides well with the experimental data. Therefore it lays a solid foundation for the practical application of the technology.

2. The basic rigid-plastic FEM equations

In this paper, the rigid-plastic FEM method had been adopted to analyze the stress and strain distribution of the forming process of composite tubes by LISSE. Firstly, the deformation body was dispersed with the quadrangle element with four nodes, and the nonlinear equations for the nodal velocity were linearized and solved by the Newton-Rapson iterative method. Then the whole matrix equations of rigid-plastic FEM can be gained by integrating all the elements [8].

$$[S]_{n-1}\{\Delta u\}_n = \{R\}_{n-1} \tag{1}$$

where, $[S]_{n-1}$ is the coefficient matrix, $\{\Delta u\}_n$ is the velocity increment, $\{R\}_{n-1}$ is the nodal residual stress.

The analysis of the temperature fields of the LISSE forming process is regarded as the non-stable heat transfer problem with internal heat source. By making discrete and then adopting the Galerkin differential method, which converges in any case, the basic finite element equation to solve the non-stable temperature field [9] is derived as following:

$$[A][T]^t = [P0]^t + [A0][T]^{t-\Delta t} + [Q0 \cdot \Delta S] \tag{2a}$$

$$[A] = 2[K] + \frac{3[C]}{\Delta t} \tag{2b}$$

$$[A0] = \frac{3[C]}{\Delta t} - [K] \tag{2c}$$

$$[P0] = 2[P0]^t + [P0]^{t-\Delta t} \tag{2d}$$

where, $[K]$ is the general heat transfer matrix, $[C]$ is the general heat capacitance matrix. Both $[K]$ and $[C]$ are the sparse band matrix in symmetrical and positive definite form. $[P0]$ is the general heat current column matrix, $[Q0 \cdot \Delta S]$ is the average speed rate column matrix of crystallization latent heat released by the nodes with phase transforming.

3. The quasi-coupling thermal-mechanical analysis method and the technical handling

3.1. The quasi-coupling thermal-mechanical calculation mode

For the coupling thermal-mechanical calculation, the material deformation has an influence on the boundary conditions such as heat transfer and the convective radiation, and most of the plastic work generated by the deformation will turn into heat energy, and the change of the temperature will result in the change of the yield stress and some other parameters related to the temperature. Meanwhile, thermal expansion gives rise to thermal stress and thermal strain either. In this case, some corresponding treatment ought to be done in numerical simulation.

Because the LISSE process is related with the transition from liquid phase to solid phase and large plastic deformation, it is difficult to set up the mathematic model via the complete coupled calculation between the deformation and the temperature. The quasi-coupling thermal-mechanical method is adopted in this paper, namely, the deformation and the temperature are two independent systems and calculated respectively, and the coupled terms (the terms affecting temperature when calculating the deformation, and the terms affecting deformation when calculating the temperature) are handled as corresponding "load". The calculation model is shown as below:

(1) Solving the initial temperature fields by formulae (2) according to the initial heat parameters and thermal boundary conditions.

(2) Solving the velocity field that corresponds to the initial temperature field according to the initial deforming conditions.

(3) Modifying the character parameters of the material according to the particular temperature fields at the corresponding moment, and handling the dynamic boundary condition and calculating the real velocity fields by the New-Raphson iterative method.

(4) Working out the strain rate of every node in the deformation body according to the velocity fields, followed by working out the stress fields according to the constitutive relation, and then deciding whether it is necessary to re-mesh the deformation grids after the nodal coordinate and related parameters being renewed.

(5) Exerting pressure on the deformation body and calculating the temperature fields at the next moment.

(6) Repeating the procedures (3) to (5) until the deforming degree meets the demand.

3.2. The handling of the liquid phase zone in the deformation body

According to the stress state characteristic of the liquid-solid forming under high pressure [10], the internal unsolidified liquid metal is in isostatic state (Fig. 2).

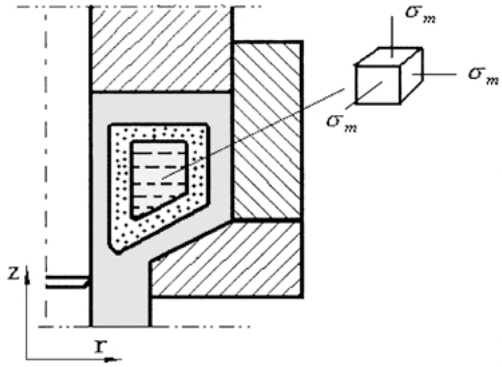

Figure 2 The scheme of liquid phase and solid-liquid phase existed in the deforming body.

Although the liquid metal will vary from liquid phase and/or semi-solid phase to solid phase as the temperature lowering, and the shape of liquid metal remained will change with the process going, the shearing stress is zero at a certain moment. Therefore, the liquid metal can be treated as rigid zone. Furthermore, the transition zone, namely the solid-liquid phase zone between liquid phase zone and solid phase zone, should be taken into account when the theoretical mode is established, otherwise the simulation value of this zone will be an abrupt change. As a result, the effect of temperature on the flow stress has been considered at the time of setting up the constitutive relation between strain and stress in this paper, which has been taken as the simple exponential function relation [11] as following:

$$\sigma = k\varepsilon^{\mathrm{m}} \tag{3}$$

Considering the differences among the liquid phase, solid-liquid-phase and solid phase, the k, m were given for different constants at different phase zone to avoid the trouble and difficulty resulted from adding the external restriction, to make the establishment of the numerical model easy, and at the same time to shorten the calculation time. Moreover, the result obtained by adopting this method is acceptable as soon as the increment interval is small enough. The simulation result shows that this handling method meets our precision demand.

3.3. The handling of the latent heat of crystallization

During the LISSE process, the latent heat of crystallization will be released continually when the liquid metal turns into solid metal. In this paper, it is handled by the method of equivalent specific heat [12]. Supposing C_{cE} expresses the equivalent specific heat of the composite material, and V_{f} is the fiber volume fraction, then

$$C_{\mathrm{cE}} = C_{\mathrm{m}}(1 - V_{\mathrm{f}}) + C_{\mathrm{p}}V_{\mathrm{f}} - L_{\mathrm{c}}\frac{\partial f_{\mathrm{s}}}{\partial T} \tag{4}$$

where, $\frac{\partial f_{\mathrm{s}}}{\partial T}$ can be derived from Scheil equation [13], that is:

$$\frac{\partial f_{\mathrm{s}}}{\partial T} = \frac{1}{K-1}\left(\frac{T_{\mathrm{m}} - T}{T_{\mathrm{m}} - T_{\mathrm{L}}}\right)^{\frac{1}{K-1}-1} \cdot \frac{1}{T_{\mathrm{m}} - T_{\mathrm{L}}} \tag{5}$$

where, K is the distribution coefficient of the metal; T_{m} is the solidus curve temperature of the matrix metal; T_{L} is the liquidus temperature of the metal; the suffix c, m, p denote the composite material, matrix metal and preform respectively.

3.4. The handling of the boundary condition

3.4.1. The friction boundary condition

The handling of the friction boundary condition is the foundation to assure the accurate simulation calculation. In this paper, the arc tangent function friction model has been adopted [8], the friction force f on the contacting surface between deformation body and the extrusion mould is shown as below:

$$f = -mk\left\{\frac{2}{\pi}tg^{-1}\left(\frac{v_{\mathrm{n}}}{\alpha}\right)\right\}\vec{t} \tag{6}$$

where, m is the friction factor, k is the shearing yield stress, v_{n} is the relative slip velocity on the contacting surface between the deformation body and the mould, α is the positive constant in some orders of magnitude smaller than the slip velocity and has been defined as 10^{-5} here, and $\vec{t}$ is the unit vector of the relative slip velocity on the contacting surface.

3.4.2. The handling of the dynamic boundary condition

The rigid-plastic FEM is calculated by loading incrementally. At each step of the incremental loading, some nodes fall under the restriction of the mould because they turn to contact with the mould surface and some nodes turn to be the free due to the deviation from the mould at the same time, i.e., the restriction condition continually varies along with the deformation process. Apparently, the dynamical boundary should be handled during the rigid-plastic FEM simulation.

For handling the dynamical boundary condition, first of all, the boundary information should be input, the contacting nodes are exerted the velocity restriction in the normal direction and the friction force in the tangential direction. Then the real stress states of the deformation body are idealized as the mechanical model that is easy to calculate, for example, exerting the velocity restriction on the nodes, simplifying the friction force as equivalent nodal force. What is more, the boundary information will change correspondingly with the number of boundary nodes after each step of extrusion.

3.4.3. The handling of slope boundary

In order to exert restriction condition on the contacting boundary nodes located at the slope surface of the forming die, a local coordinate system is constructed by using a τ-, n-pair to specify the normal and tangential direction of the die respectively (Fig. 3). The parameters of the integral coordinate system turn into the local coordinate system for calculation. The convert matrix

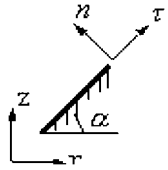

Figure 3 The scheme for the coordinates conversion.

for the node i is shown as below:

$$[T]_{\mathrm{i}} = \begin{bmatrix} \cos\alpha & \sin\alpha \\ -\sin\alpha & \cos\alpha \end{bmatrix} \tag{7}$$

where, α is the rotation angle required to superimpose the x axis on the τ axis and has the positive value at anticlockwise rotation.

If there are k contacting nodes in all, the converting matrix from integral coordinate system to the local coordinate system is shown as below:

$$[T] = \begin{bmatrix} [T]_{\mathrm{l}} & 0 & 0 \\ 0 & \cdots & 0 \\ 0 & 0 & [T]_{\mathrm{k}} \end{bmatrix} \tag{8}$$

In the $\tau - n$ local coordinate system, it is easy to exert the normal velocity restriction on the nodes in the slope surface. The velocity increment column matrix in the local coordinate system is worked out by adopting the Newton-Raphon iterative method repeatedly. Then, by converting it inversely, the velocity increment in the integral coordinate system is worked out accordingly.

3.5. The transform of plastic deformation energy to internal heat source

As mentioned above, the plastic deformation energy of solid or semi-solid metal tended to transform into the heat, elevating the temperature of deformation body and furthermore changing the mechanical behaviors of the materials. Evidently, it is essential to calculate the plastic deformation energy. In present paper, the plastic deformation energy was determined by the formula (9):

$$\pi = \int \sigma_{\mathrm{s}} \dot{\bar{\varepsilon}} \, \mathrm{d}v \tag{9}$$

Transform it into internal heat source of temperature field, we get

$$Q_{\mathrm{v}} = \beta \cdot \pi \tag{10}$$

where σ_{s} represented the flow stress of Al_2O_{3sf}/$AlCu_5Mg_2$ composite in a semi-solid state under high temperature and could be determined by the element temperature. The denotation β was a coefficient ranged from 0.8 to 0.9.

3.6. The re-meshing grid technique

The grids gradually distort in the LISSE process. The calculating precision will be affected by taking the distorted grids as the referential state in the process of the increment calculation. The calculating result is not convergent, even the calculation can't be carried out any more. Thus the calculation should be stopped and the grids should be re-meshed when the grid distortion reaches a certain degree.

For a quadrangle element, when the Jacobi matrix $|\mathrm{J}| \leq 0$, namely the interior angle of a quadrangle is bigger than 180°, the quadrangle loses its convex property, the grid should be re-meshed. Even when the interior angle is less than 180°, the calculation is not precise enough. In the practical usage, the judgment rule is described as following:

$$30^\circ \leq \theta_{\mathrm{i}} \leq 150^\circ \quad (i = 1, 2, 3, 4) \tag{11}$$

where, θ_{i} is the interior angle of a quadrangle. It is thought that the grid has distorted badly when the interior angle doesn't satisfy the rule (11), meaning the grid needs to be re-meshed.

At present, the adaptive generating grid technique without the manual intervention is not mature yet, in most cases, the generating grid process needs manual intervention, and the general method is related with the certain process. Whatever the generating method is adopted, the generated grid system should keep the boundary shape of the deformation body and the contacting condition with the mould unchanged, the element of the new grid system should be as possibly same as the original element in shape, the four interior angles should be about 90° and the calculation workload of the matrix should be the smallest.

Based on the demand of the calculation process, the manual intervention method is adopted, moreover, the element number of the new grid system and the original grid number remain unchanged in this paper. In order to improve the calculation precision, the grids inside the forming die have been meshed relatively smaller because the interior part of the forming die is the main deformation zone in the LISSE process.

After the grid being re-meshed, the information of the old grid system should be transferred to the new grid system for the continuation of the analysis. In this paper, the direct transfer method [14] has been adopted. Based on the coordinate values of the nodes in the new grid system, their locations in the old grid system are directly determined. Then the information transfer is carried out. Because the values of some field variables are output in the center of the grid, so the value in the center of the grid must be converted to the node by interpolation before the information transfer. In this paper, the area-weighted average method has been adopted, which is explained by the example of equivalent strain as below.

Assuming that node n is located on the boundary of m grids, then the area of the related grids is dealt as weight, and the strain average value is worked out, which is taken as the strain value $\overline{\varepsilon_{\mathrm{n}}}$ of the node n.

$$\overline{\varepsilon_{\mathrm{n}}} = \frac{1}{\sum_{\mathrm{s}} A_{\mathrm{s}}} \sum_{\mathrm{s}} A_{\mathrm{s}} \overline{\varepsilon_{\mathrm{n}}} \tag{12}$$

where, $\overline{\varepsilon_{\mathrm{n}}}$—the equivalent strain of the grids around the node, A_{s}—the element area around the node,

TABLE I Material parameters in the analysis

Materials	Density ρ (g/mm^2)	Specific heat c_p (J/g · °C)	Heat transfer coefficient λ (W/m · °C)
$AlCu_5Mg_2$ alloy (liquid)	2.35×10^{-3}	1.08	91.9
$AlCu_5Mg_2$ alloy (solid)	2.66×10^{-3}	0.99	228.6
Al_3O_2 short fiber	3.40×10^{-3}	1.05	3.98
Mould material	7.85×10^{-3}	0.517	48.1

and $\sum_s$—the sum of the all elements around the node.

3.7. The parameters for numerical simulation

The material parameters of numerical simulation for the LISSE process are listed in Table I. The solidus of matrix metal T_m takes 630°C, and the liquidus T_L is 580°C. The latent heat of crystallization L_c takes 387.5 kJ/kg.

4. The simulation result and the analysis

Based on the model established above, a rigid plastic FEM simulation system software, including the solidification, heat transfer and large plastic deformation for forming composite tubes by LISSE, has been developed by the authors. The system software consists of three parts, the pre-handling module, the deformation analytic module and after-handling module. By the software, the grids are automatically meshed according to the requirement, the temperature fields, stress-strain fields and deformation pressure are simulated, as well as the nodal information at each moment is visualized.

The simulated results of temperature, equivalent stress and equivalent strain distribution at different moment for the $AL_2O_{3sf}/AlCu_5Mg_2$ composite tube by LISSE are illustrated in the Figs 4 and 5. It can be seen from the figures that the equivalent strain value is bigger at the slope surface of the forming die and especially so in the round corner, where the stress value is bigger too. Nevertheless the strain value is lower in the extrusion container, where there is no large plastic deformation basically. The equivalent strain in the part extruded out but near the outlet of the forming die is bigger and becomes smaller in the further part. This is mainly because the material at the outlet of the forming die just undergoes much large plastic deformation, but after that, no deformation exists and the workpiece can be seen as rigid zone. When the extrusion process nears to finish, the material becomes in solid state completely, causing both the deformation and the stress value larger in the extrusion container (Fig. 5).

According to simulation, there still exists the unsolidified liquid metal in the extrusion container at the beginning period of the process. The certain isostatic pressure borne by the liquid metal leads the liquid metal to crystallize and solidify under pressure and to feed shrinkage forcedly. This is helpful for improving the interface bonding between the matrix material and the reinforcing fiber, and contributing for a better microstructure of the workpiece. Then the material gets into the deforming area and bears the friction pressure on the slope surface of the forming die, the large plastic deformation, and the shearing deformation. The crystal grain will be further crushed, and the property of the workpiece is improved overall.

After the process is carried out to a certain period, the liquid zone wil be gradually disappeared with the temperature decreasing, the deforming behavior in the still existed solid-liquid zone and the solidified zone becomes more violent. So the strengthening by the plastic deformation and the shearing deformation persists during the whole process.

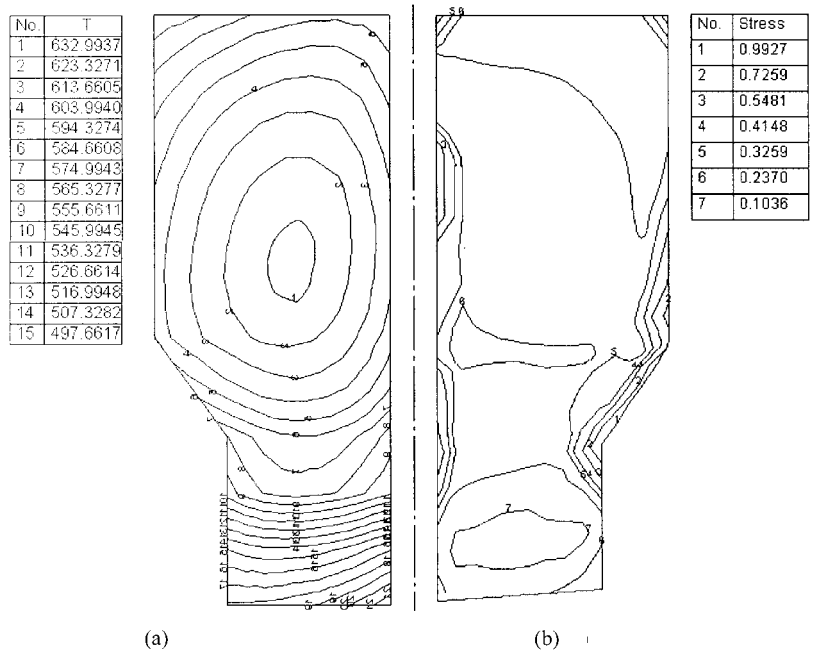

Figure 4 The temperature and equivalent stress distribution when the pressing amount is 20%: (a) temperature distribution (°C) and (b) the equivalent stress distribution (×10 MPa).

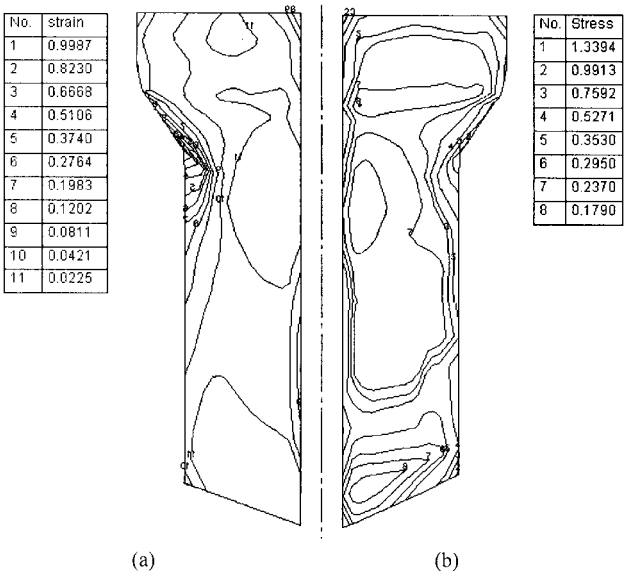

Figure 5 The equivalent strain and stress distribution when the pressing amount is 80%: (a) the equivalent strain distribution and (b) the equivalent stress distribution ($\times$10 MPa).

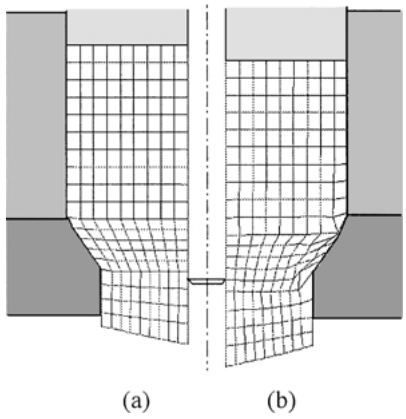

Figure 6 The grid change before and after the second re-meshing: (a) new grids re-meshed after and (b) the distorted grids before the second re-meshing.

Since the strain value at the round corner of the forming die is bigger, the grids in this zone will be distorted rapidly. So the grids need to be re-meshed frequently in the deformation course to achieve a precise numerical simulation. In this paper, the grids had been re-meshed for 11 times in the simulation process.

Fig. 6 shows the comparison for the grid distortion in the extrusion process. It is clear that the grid deformation on the slope surface of the forming die is more serious while the grid deformation at the border between the extrusion container and the forming die is in the most severe degree. The reason is that the flow direction of the material changes at the corner due to the friction produced as soon as the grids contact with the slope surface of forming die. Besides, it is also found from the figure that the flow of the right part of the workpiece is slow because of friction (Fig. 6b), so the exterior surface of the workpiece undergoes some tensile stress, the workpiece will break at surface if the tensile stress exceeds the intensity limit.

The comparison of the grids before and after the 10th re-meshing is shown in Fig. 7. It can be seen that the

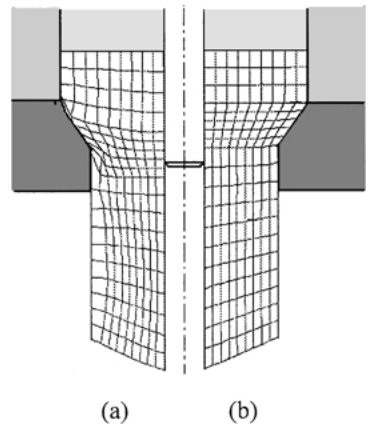

Figure 7 The comparison before and after the 10th grid re-meshing: (a) the distorting grids and (b) the grids after re-meshed.

moving restriction of some nodes has been changed in the extrusion process because of the large deformation degree. Some free nodes become into the contacting nodes with the forming die. In this moment, it is needed to do some corresponding modification on the coordinate value, velocity value and the mark information of the nodes. In this paper, the nodes are supposed to enter the die's body firstly, and then they are extracted back to the slope surface along the normal direction of the die surface. The error brought by the modification is definitely small because the deformation increment of every step is very small, so it can meet the engineering accurate demand.

Fig. 8a shows the relationship between the deforming pressure and the extrusion increment step in the LISSE process. It can be seen that the extrusion pressure is increased continually along with the displacement increment after the extrusion begins, and then enters into a steady period and the extrusion pressure becomes relative calm after it reaches 1.7 MN. This is because the liquid phase becomes less and less in the extrusion process and the deforming pressure must be gradually increased for maintaining the deformation of solidified zone. The steady period of the pressure is the result of the balance between the reducing rate of liquid phase area and the extruding rate of the workpiece. At the last period, the deforming pressure increases rapidly again to 1.9 MN, the reason is that the remained metal has fully solidified and there is no liquid metal left, so the deforming pressure must become bigger. The simulation curve is basically coincided well with the experimental curve of $Al_2O_{3sf}/AlCu_5Mg_2$ composite (Fig. 8b), except in the late period of the deformation, the extrusion pressure measured by experiment drops a little larger than that by simulation, this may be resulted by the change of the real friction coefficient along with temperature continually, while the friction coefficient has been regarded as a constant in the numerical simulation. This can be testified by Fig. 9, which shows the varying curves of the extrusion pressure with different frictional coefficients. The extrusion pressure increases correspondingly when the friction coefficient increases. Many experiments approve that the simulation result is coincident well with the practical situation and the extrusion pressure varies among

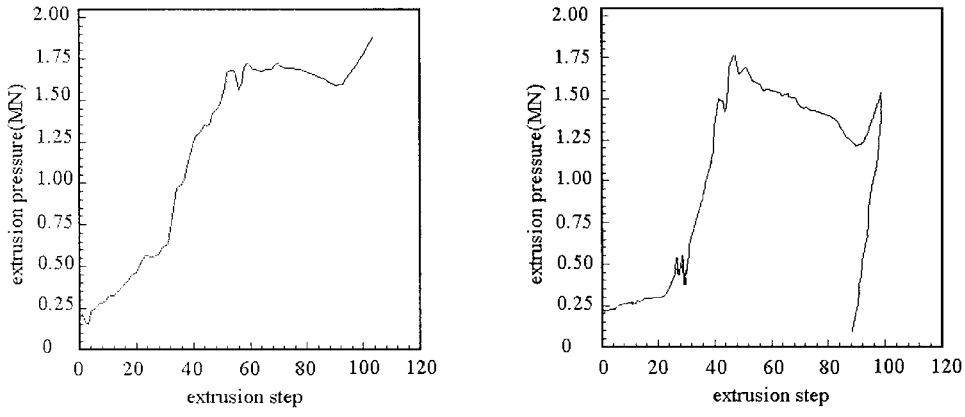

Figure 8 The relative curve between the deforming force and the extrusion increment step: (a) the numerical simulation curve and (b) experimental curve.

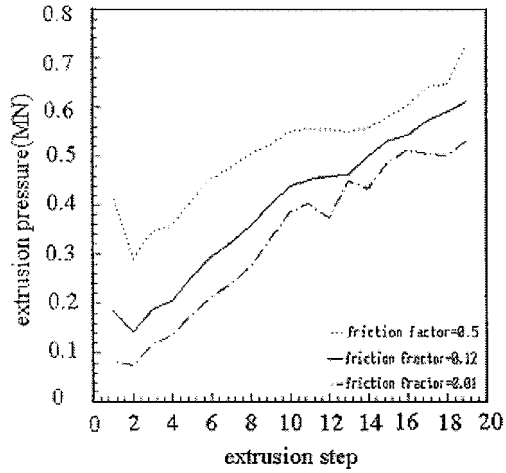

Figure 9 The deforming force changing curves with different friction condition.

1.5 MN–1.8 MN and goes up to 1.9 MN when the extrusion process is over. This indicates that the simulation system is feasible.

5. Conclusions

Based on the rigid plastic FEM principle, a rigid plastic quasi-coupling thermal-mechanical FEM model for the LISSE process is established to solve some technical difficulties in the simulation process. By developing the simulation software, the temperature fields, the stress-strain fields and the deforming pressure of the composite tubes formed by the LISSE process have been obtained. The simulation results are coincident well with the experimental data, laying a theoretic foundation for the practical use of this technology.

Acknowledgement

The authors wish to express their sincere thanks to the National Nature Science Foundation of China (50175091) and Innovation Foundation by Northwestern Polytechnical University for providing financial supports.

References

1. M. R. GHOMASHCHI and A. VIKHROV, *J. Mater. Process. Tech.* **101** (2000) 1.
2. J. HASHIM, L. LOONEY and M. S. J. HASHMI, *ibid.* **92/93** (1999) 1.
3. V. M. KENORKIJIAN and B. SUSTARSIC, *Key Engineering Materials* **127–131** (1997) 471.
4. LEHUA QI, LEMIN SUN, JUNJIE HOU and HEJUN LI, *J. Northwestern Polytech. Univ.* **17**(4) (1999) 629.
5. Y.-M. GUO, K. NAKANISHI and Y. YOKOUCHI, *J. Mater. Process. Tech.* **89/90** (1999) 111.
6. M. PIETRZYK, *ibid.* **106** (2000) 223.
7. YUNSHENG SHI and JINXIANG DONG, *Chinese J. Appl. Mech.* **16**(4) (1999) 78.
8. LIPING LU, The Finite Element Method and Its Application in Forging Engineering. (Northwestern Polytechnical University Publishing House, Xian, 1989).
9. GAOTIAN LIU, "The Numerical Simulation of the Temperature Fields" (Chongqing University Publishing House, Chongqing, 1990) p. 20.
10. LI HEJUN, QI LEHUA, LUO SHOUJING *et al.*, *J. Mater. Process. Tech.* **30**(3) (1992) 287.
11. SUN JIAKUAN and LUO SHOUJING, *The Chinese Journal of Nonferrous Metals* **9**(3) (1999) 493.
12. GUOHONG XIE and SONGCHUN LI, *Hot Working Technology* **2** (1995) 5.
13. HANQI HU, "The Solidification Principle of the Metal" (Mechanical Industrial Publishing House, 1991) p. 66.
14. HAINAN HAO and YAN LU, *Metal Forming Technology* **5**(3) (1997) 180.

Received 7 May 2002
and accepted 10 June 2003